MATHEMATICAL BIOSCIENCES
AND ENGINEERING
Volume **12**, Number **4**, August **2015**

doi:10.3934/mbe.2015.12.841

pp. **841–858**

QUANTITATIVE IMPACT OF IMMUNOMODULATION VERSUS ONCOLYSIS WITH CYTOKINE-EXPRESSING VIRUS THERAPEUTICS

Peter S. Kim

School of Mathematics and Statistics
University of Sydney
Sydney, NSW, Australia

Joseph J. Crivelli

Weill Cornell Medical College
New York, NY, USA

Il-Kyu Choi and Chae-Ok Yun

Department of Bioengineering
College of Engineering
Hanyang University
Seoul, South Korea

Joanna R. Wares

Department of Mathematics and Computer Science
University of Richmond
Richmond, VA, USA

Abstract. The past century's description of oncolytic virotherapy as a cancer treatment involving specially-engineered viruses that exploit immune deficiencies to selectively lyse cancer cells is no longer adequate. Some of the most promising therapeutic candidates are now being engineered to produce immunostimulatory factors, such as cytokines and co-stimulatory molecules, which, in addition to viral oncolysis, initiate a cytotoxic immune attack against the tumor.

This study addresses the combined effects of viral oncolysis and T-cell-mediated oncolysis. We employ a mathematical model of virotherapy that induces release of cytokine IL-12 and co-stimulatory molecule 4-1BB ligand. We found that the model closely matches previously published data, and while viral oncolysis is fundamental in reducing tumor burden, increased stimulation of cytotoxic T cells leads to a short-term reduction in tumor size, but a faster relapse.

In addition, we found that combinations of specialist viruses that express either IL-12 or 4-1BBL might initially act more potently against tumors than a generalist virus that simultaneously expresses both, but the advantage is likely not large enough to replace treatment using the generalist virus. Finally, according to our model and its current assumptions, virotherapy appears to be optimizable through targeted design and treatment combinations to substantially improve therapeutic outcomes.

2010 *Mathematics Subject Classification.* Primary: 92C50, 92B05; Secondary: 37N25.

Key words and phrases. Oncolytic virotherapy, adenovirus, cytokines, co-stimulatory molecules, mathematical model, ordinary differential equations model.

1. **Introduction.** Many cancers are unresponsive to conventional therapies, necessitating the development of novel approaches, such as oncolytic virotherapy. Oncolytic viruses selectively infect and kill tumor cells while sparing normal tissues [30]. Replication in cancer cells leads to long-term local amplification of the therapeutic agent.

Consistent with this effect, many oncolytic viruses are designed as gene-delivery vectors. Among the most promising strategies is the genetic engineering of oncolytic viruses which foster expression of pro-inflammatory cytokines and co-stimulatory molecules that induce a targeted immune attack against the tumor [13, 27]. This approach counteracts immune evasion by the tumor, one of the hallmarks of cancer [16], and can produce a robust anti-tumor effect when coupled with viral oncolysis.

Historically, several cancers (e.g. melanoma and non-muscle-invasive bladder cancer (NMIBC)) have been very responsive to immunotherapy, making them excellent targets for therapy with cytokine- and/or costimulatory-molecule-expressing oncolytic viruses [24, 38]. Importantly, the relative contributions of the immunomodulatory and oncolytic activities of these oncolytic viruses to cancer killing are largely unknown.

There is also no consensus on the optimal choice of immunomodulatory genes for expression by a particular viral vector. While evidence suggests that two different oncolytic viruses can be rationally combined to produce a synergistic cancer-killing effect [23, 31, 41], co-expression of two or more such genes within a single oncolytic virus is routinely attempted. However, combination therapy with two or more oncolytic viruses, expressing distinct cytokines or cosimulatory molecules, has not been reported. Unfortunately, in vivo experiments to quantify immunomodulatory and oncolytic behavior and compare possible gene expression combinations are costly and not always feasible.

Mathematical modeling of oncolytic virotherapy and cancer immunotherapy using systems of differential equations can improve the design and administration of these treatments, especially when experimental data are incorporated [12, 20, 36, 37]. Recent examples of such studies include the model-based development of optimized treatment schedules for measles virus [5]; interferon-evasion mechanisms for vesicular stomatitis virus (VSV) [22]; ideal combinations of adenovirus infection and MEK inhibition [2]; and personalized prostate cancer vaccine regimens [21].

In addition to offering a cost-effective and practical approach to understanding the efficacy of virotherapy and immunotherapy, mathematical models also have the ability to reveal dynamic patterns that govern therapeutic potency and efficacy. Such mathematically-derived biological insights include the basis for oscillations in the response of myeloma to measles virus [11], the impact of initial melanoma tumor size on outcomes of VSV therapy [29], factors that inhibit and enhance herpes simplex virus spread through a tumor[28], and the limited capacity of the innate immune response to bacillus Calmette-Guérin therapy for NMIBC [6]. Several mathematical models have also been used to investigate the complex dynamics that arise between tumor cells, oncolytic viruses, and the immune system [35, 40].

Here, we formulate a mathematical model of therapy with oncolytic viruses that simultaneously express immunostimulatory cytokines and cosimulatory molecules. Given that the use of cytokine-expressing oncolytic viruses is advancing in clinical settings, the development and validation of mathematical models describing their mechanisms is warranted.

For our study, we developed systems of ordinary differential equations (ODEs) to predict the dynamics of tumor treatment with oncolytic adenovirus expressing the costimulatory molecule 4-1BB ligand (4-1BBL) and cytokine interleukin-12 (IL-12). Model parameters were obtained by fitting model trajectories to murine tumor volume data. We then simulated the model to investigate the possible effects of different oncolytic viruses in isolation and in combination.

2. **Model and fit.** We developed a mathematical model to predict changes in tumor size in response to treatment by various types of oncolytic adenoviruses that are expressing immunostimulatory molecules. The four adenoviruses that we consider are adenovirus alone, adenovirus expressing 4-1BBL, adenovirus expressing IL-12, and adenovirus co-expressing 4-1BBL and IL-12. We then fit the parameters of the model to previously published murine tumor growth data [17] which was recorded daily. Each data set represented average tumor growth for 8-9 mice. All data sets contained measurements of murine B16-F10 melanoma tumor volumes with respect to time [17].

2.1. **Model equations and assumptions.** Our mathematical model for adenovirus co-expressing 4-1BBL and IL-12 (generalist virus) is given by the ODE system:

$$\frac{dU}{dt} = rU - \beta\frac{UV}{N} - k(I)\frac{UT}{N} \tag{1}$$

$$\frac{dI}{dt} = \beta\frac{UV}{N} - \delta_I I - k(I)\frac{IT}{N} \tag{2}$$

$$\frac{dV}{dt} = u(t) + \alpha\delta_I I - \delta_V V \tag{3}$$

$$\frac{dT}{dt} = s_T(I) + pA - \delta_T T \tag{4}$$

$$\frac{dA}{dt} = s_A(I) - \delta_A A \tag{5}$$

A diagram of model dynamics is given in Figure 1. Models for the other adenoviruses can be obtained by setting appropriate parameters to zero. Here, U is the number of uninfected tumor cells, I is the number of infected tumor cells, V is the number of virions, T is the number of T cells at the tumor site, A is the number of APCs at the tumor site, and $N = U + I + T + A$ is the total cell population (excluding virions) at time t. The biological mechanisms modeled by equations (1) - (5) are described as follows:

- Frequency-dependent transmission rates are utilized by dividing each transmission term by N. For instance, in the term $k(I)\frac{UT}{N}$, T cells make contact with U cells at a rate that is dependent on the total number of U cells in the population U/N. The population N represents the total population of cells at the tumor site. Our choice of frequency-dependent term reflects our assumption that viruses remain predominantly localized to the tumor site and thus almost exclusively interact with cells at the tumor site as opposed to elsewhere. (An alternative assumption is that viruses only interact with tumor cells at the site, in which case, we would use $N = U + I$. However, we found in our simulations that the T cell and APC populations, T and A, were always so much lower than the total tumor population this alternative choice of N hardly makes a difference in the model's dynamics.)

- In equation (1), uninfected tumor cells, U, grow at rate of r. Although not the most realistic model of tumor growth, exponential growth is a sensible assumption here since the data was collected for the short time period of 30 days and we run our simulations for at most 60 days [37]. Virions, V, infect uninfected cells at a frequency-dependent rate with infection parameter β. T cells, T, at the tumor site kill uninfected cells at a frequency-dependent rate with parameter $k(I)$, where I is the number of infected cells.
- In equation (2), $\beta\frac{UV}{N}$ is the rate at which tumor cells become newly infected. Infected cells lyse at rate δ_I and, like uninfected cells, are killed by T cells at a frequency-dependent rate.
- In equation (3), $u(t)$ is the rate at which new virions are injected into the system at time t, which is determined by the treatment protocol. Upon lysis of each infected cell, α new virions are released and free virions are cleared or inactivated at rate, δ_V.
- In equation (4), 4-1BBL provides a co-stimulatory signal to activate T cells at a rate of $s_T(I)$. In the presence of IL-12, additional T cells are also activated by APCs at rate p. T cells die at a rate of δ_T.
- In equation (5), IL-12 stimulates recruitment of mature APCs to the tumor site at a rate of $s_A(I)$, and APCs die at rate of δ_A.

The major assumptions and conditions of the model are the following:

1. Virus-infected cells produce 4-1BBL, which promotes T cell differentiation and cytotoxicity. We assume that the amount of 4-1BBL produced, and therefore the T cell supply rate and T cell killing rate, are proportional to the number of infected cells, I, i.e. $s_T(I) = c_T I$ and $k(I) = c_k I$, where c_k and c_T are constants.
2. Virus-infected cells produce IL-12 which increases APC recruitment and T cell cytotoxicity. We assume that the APC supply rate, $s_A(I) = c_A I$, is also proportional to the number of infected cells and that IL-12 production also affects $k(I)$.
3. The variables T and A represent T cells and APCs recruited by virus-mediated 4-1BBL and/or IL-12. We assume that the baseline immune response is already factored into the net tumor growth rates.
4. While IL-12 can stimulate the innate immune response (e.g. natural killer cells), we only consider its effect on the cytotoxic T cell response [10], and we do not explicitly model an immune response, e.g, antibody response, to the virus itself.
5. We assume that all populations start at size 0, except for the initial population of uninfected tumor cells, $U(0)$, whose size is equivalent to the experimental measurement of tumor size at time 0.
6. In Huang et al. [17], tumor size is measured by volume (mm^3). In our model, it is measured by number of cells, $U + I$ as in our model. To convert between volume and cell number, we assume tumor cells have a diameter of approximately 0.01 mm [1, 7, 26], and hence occupy a volume of order $10^{-6}mm$, meaning that 1 mm^3 contains on the order of 10^6 tumor cells. The same system of equations could be obtained without such scaling, but the scaling is done to more easily describe our results in units consistent with those of the experiments.

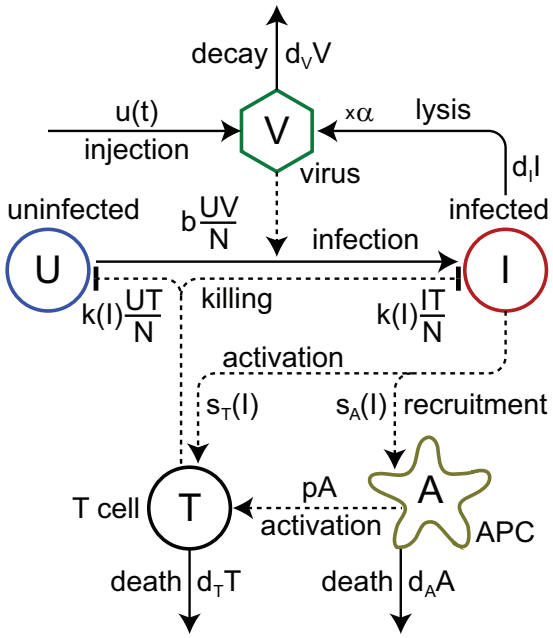

FIGURE 1. Diagram of the model of tumor-virus dynamics. Virus is injected into the system at times determined by the treatment protocol. Viruses infect uninfected tumor cells. Infected tumor cells lyse and produce more virions. Infected cells also activate T cells and recruit APCs. APCs activate T cells, and T cells kill uninfected and infected tumor cells.

2.2. **Model fitting.** Before fitting the model to data, we estimate six of the parameters based on other information from experimental literature. We estimate that oncolytic adenovirus produces a viral burst size of $\alpha = 3500$ [8]. The time for infected cells to undergo lysis is on the order of 1 day, $\delta_I = 1/day$, which corresponds to an average lysis time of one day [3, 14, 15, 18]. Ninety percent of viruses decay or exit the tumor site in one day [39]. Accordingly, we estimated a viral decay rate of $\delta_V = -\log ?10\%) = 2.3/day$, which also agrees with the decay rates of Li et al. and Wang et al. [25, 34]. We estimated that T cells have a half-life of 48 hours, so that $\delta_T = 0.35/day$ as shown in [9]. We assumed that APCs die or exit the system at a similar rate as T cells, yielding an APC death rate of $\delta_A = 0.35/day$. We also assumed that, at baseline, APCs activate a T cell in an average time of 1 day, so that $p = 1/day$ [32, 33]. These parameter estimates are summarized in Table 1.

To estimate the other model parameters, we fit the model equations (1) - (5) to experimental data that measured tumor growth over time during treatment by oncolytic adenoviruses. The data was collected under five conditions: (i) control, or phosphate buffered saline (PBS), (ii) adenovirus, (iii) adenovirus expressing 4-1BBL, (iv) adenovirus expressing IL-12, and (v) adenovirus co-expressing 4-1BBL and IL-12, [17, Fig. 2a]. Tumor growth was recorded daily and represented the average of 8-9 mice. All data sets contained measurements of murine B16-F10 melanoma tumor volumes with respect to time [17].

For each of the five cases above, we assumed the tumors start at the size measured at time 0, i.e., (i) 73.7, (ii) 59.2, (iii) 62.4, (iv) 74.6, and (v) 59.3 mm^3. In addition,

Parameter and Description		PBS	Ad	Ad/ 4-1BBL	Ad/ IL-12	Ad/4-1BBL /IL-12
r	Net tumor growth (day^{-1})	0.31	0.31	0.31	0.31	0.31
β	Infection rate (day^{-1})	-	8.9×10^{-4}	8.9×10^{-4}	8.9×10^{-4}	8.9×10^{-4}
c_k	Kill const. (cell^{-1} day^{-1})	-	-	1.5×10^{-7}	6.7×10^{-7}	8.5×10^{-7}
c_T	T cell constant (day^{-1})	-	-	2.9	-	1.28
c_A	APC constant (day^{-1})	-	-	-	1.44	0.22
α	Viral production	-	3500	3500	3500	3500
δ_I	Infected lysis (day^{-1})	-	1	1	1	1
δ_V	Viral decay (day^{-1})	-	2.3	2.3	2.3	2.3
δ_T	T cell decay (day^{-1})	-	-	0.35	0.35	0.35
δ_A	APC death (day^{-1})	-	-	-	0.35	0.35
p	T cell-APC rate (day^{-1})	-	-	-	1	1

TABLE 1. Parameter estimates used in the model equations (1) - (5). We fit the top five parameters to the data. We estimate the bottom six parameters based on other information and fix these values during fits.

we simulated the injection of three doses of (ii) 10^{10} virions, (iii) 10^{10} virions, (iv) 5×10^9 virions, and (v) 5×10^9 virions on days 0, 2, and 4, as in the experiments of [17]. Mathematically, these injections were performed by letting $u(t) = u_0(\delta(t) + \delta(t-2) + \delta(t-4))$ for $u_0 = 10^{10}$ or 5×10^9, where $u(t)$ is the rate at which new virions are injected into the system at time t and where $\delta(t)$ is the Dirac delta function.

Model parameters were fit sequentially and hierarchically by estimating parameters for submodels and retaining their values for more advanced models in accordance with progressive modifications of the base adenovirus. We numerically simulated the ODE system using the function 'ode45' in MATLAB 2011b (The MathWorks, Inc.; Natick, MA, USA) and estimated the remaining parameters by obtaining the log-least-squares fit of the model solution to data using the Levenberg-Marquadt algorithm, provided by the function 'lsqnonlin.'

For the control (PBS) data, we fit the simplest model which considers tumor growth in the absence of treatment. All other parameters were set to 0 (see the PBS column in Table 1). We estimated the net tumor growth rate, r, using a linear regression of the log-data and retained this parameter estimate for the remaining models. To fit the response of treatment with adenovirus alone, we used a model that excludes infection-induced immune response. That submodel includes the additional parameters α (viral burst size), δ_I (lysis rate of infected cells), and δ_V (viral decay rate), as estimated from the literature (see fixed parameters below), and we fit the infection parameter β to match the data for adenovirus-only treatment in [17]. For the remaining data sets, we assumed that the cytokine- and/or costimulatory-molecule-expressing viruses, Ad/4-1BBL, Ad/IL-12, and Ad/4-1BBL/IL-12, activate T cells, recruit APCs, or both, respectively, while also increasing the T cell killing rate, as indicated in the assumptions of the Models section. For all viruses, we fit the T cell killing rate, c_k. For the two viruses that mediated release of IL-12, we additionally fit the T cell recruitment rate, c_T, and for viruses that mediated release of 4-1BBL, we also fit the recruitment rate of APCs, c_A.

3. Results.

3.1. Goodness of fit.

Estimated parameters obtained through incremental fitting of our mathematical models are shown in the Table 1. Data and model solutions for all five cases are shown in Figure 2. Trajectories of tumor growth arising from

the models are extremely close to tumor growth data from the experiments. To measure the goodness of fit, we calculated the R^2 values and the Pearson r values for the model and experimental data, as well as for the log of the data. Goodness of fit values are given in Table 2. Values close to unity show good agreement between model trajectories and experimental data trajectories. For all of our submodels as well as for the full model, R^2 is above 0.94 and Pearson's r is above 0.98. Values for fits of log data are similar. In what follows, immunologic and oncolytic activities are explored with simulations of the model with the fitted parameters.

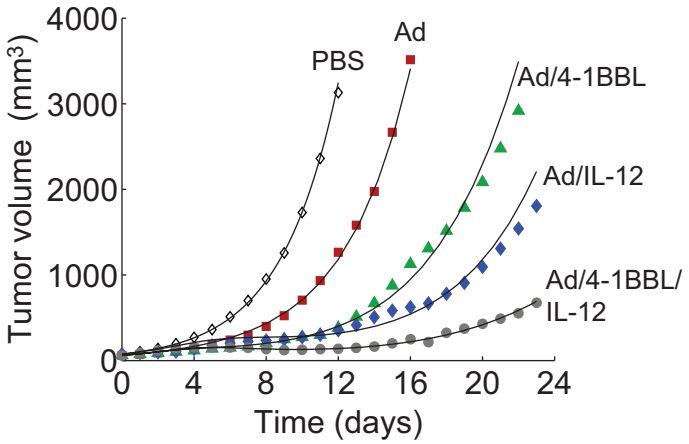

FIGURE 2. Fits of model simulations to experimental data. Experimental data correspond to Figure 2a of [17] and model solutions correspond to parameters in Table 1. We plot the tumor size in terms of volume (using conversion factor of 10^6 cells per mm^3).

Data set	R^2	Pearson's r
PBS	0.9997	0.9998
Ad	0.9959	0.9993
Ad/4-1BBL	0.9916	0.9964
Ad/IL-12	0.9483	0.9795
Ad/4-1BBL/IL-12	0.9870	0.9942

TABLE 2. Goodness of fit parameters for the model of tumor growth, tumor growth with Ad, Ad/4-1BBl, Ad/IL-12 and Ad/4-1BBL/IL-12.

As an example, Figure 3 shows numerical solutions of the system, equation (1) - (5) under treatment by Ad/4-1BBL/IL-12. As we can see from Figure 3, virus is injected on days 0, 2, and 4, causing a quick rise in the population of infected tumor cells, leading to a very slightly delayed rise in APCs and T cells. Unlike in the case of Ad (see Figure 2), the virus-induced immune response in the Ad/4-1BBL/IL-12 case begins to eliminate uninfected and infected tumors cells, which causes all other immune, virus, and infected tumor populations to fall. The immune-induced decline in infected cells and viruses ultimately leads to a tumor rebound. The dynamics in Figure 3 reveal a nonlinear, three-way race between tumor growth,

viral infection, and the virus-induced immune response. These results show that the apparent synergy from combining Ad and the immunostimulatory cytokines is not monotonic or straightforward.

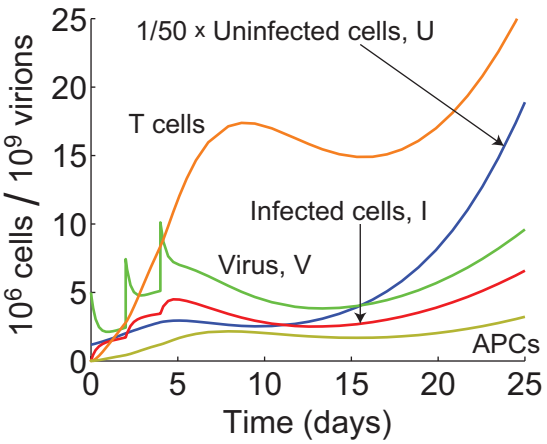

FIGURE 3. Time evolution of the system equations (1) - (5) under treatment by Ad/4-1BBL/IL-12. Populations of infected tumor cells, I, T cells, T, and APCs, A, are shown in millions, and numbers of virions, V, are shown in billions. The population of uninfected tumor cells, U, is shown at 1/50th of its value. Viruses are injected at doses of 5×10^9 on days 0, 2, and 4.

3.2. **Simulation of alternative treatment strategies.** Using model parameters from our data fits, we considered possible alternative treatment strategies and virus characteristics. For all simulations, we considered treatments using the strongest virus, Ad/4-1BBL/IL-12, shown in Figure 2 and started the tumor at an initial size of 60 mm^3 uninfected cells, which was close to the initial tumor sizes measured in Huang et al. [17].

The data from Huang et al. [17] was collected over a time interval of under 30 days, during which the tumor did not show signs of attaining a carrying capacity or maximum size. Hence, we simplified our model by assuming a constant tumor growth rate, r. Because of this simplification, we stopped simulations if the tumor size reached 3000 mm^3, which was the tumor size at which mice were killed in the experiments of [17].

3.2.1. *Varying dose periods.* We simulated the effect of varying the period between doses. Figure 4 shows the results of giving the virus in three doses of 5×10^9 virions spaced 0, 2, 4, and 6 days apart with the first dose beginning on day 0. The case with a period of 0 corresponds to injecting all three doses at once, and the case with a period of 2 days corresponds to the experimental protocol of Huang et al. [17].

From our simulations (Figure 4), we found the following: (1) more closely spaced doses cause the tumor to drop to smaller minimum sizes, (2) more widely spaced doses can delay tumor growth for longer, and (3) the tumor approaches similar long-term growth rates after treatment ends.

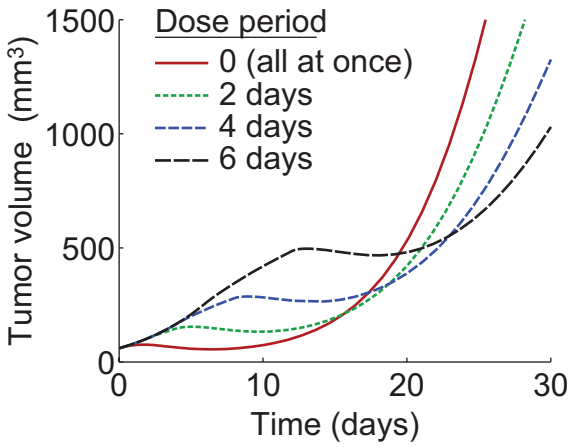

FIGURE 4. Simulations with varying dose periods. Three doses of 10^{10} virions are injected 0, 2, 4, and 6 days apart with the first dose beginning on day 0.

The long-term tumor growth rate in these simulations is essentially the same as the growth rate in the curve corresponding to Ad/4-1BBL/IL-12 in Figure 2, and is significantly slower than the growth rate in the case without virus. This result shows that the virus continues to slow tumor growth after the last dose, and the infection drives itself to a certain extent.

Our simulations reveal that the goals of killing the tumor quickly and maintaining a low population can conflict. This conflict partly occurs because the virus only replicates in infected tumor cells. Consequently a sharp decline in the tumor population will result in a subsequent drop in the virion population, allowing the tumor to rapidly rebound in the gap of time where the virus population is small. In the following sections, we report results which assess how certain modifications to the virus or treatment protocols favor a swift-kill versus slowed-growth strategy.

3.2.2. *Varying number of doses.* We simulated the effect of increasing the number of doses of virus given over the length of the experiment. Figure 5 shows tumor volume versus time when the virus is given in twelve doses of 5×10^9 virions spaced 0, 2, or 7 days apart, with the first dose beginning on day 0.

As expected, by comparing Figures 4 and 5, we see that administering more doses has a greater effect on the tumor. In addition, as also supported by the results displayed in Figure 4, administering doses closer together in time drives the tumor to smaller minimum sizes. In particular, if twelve doses are given at intervals of 0 and 2 days, tumor volume reaches minimum sizes of 4.6 mm^3 and 9.4 mm^3, respectively.

On the other hand, if the goal of the treatment strategy is to control tumor growth indefinitely, administering doses at a period of 7 days appears to eventually maintain a tumor size of under 600 mm^3 over the entire duration of the treatment. Once treatment ends, the tumor rebounds.

In contrast, giving the twelve doses all at once causes the tumor to drop to a low level, but rebound very quickly. These results imply that viral injections could be given regularly to maintain a low level tumor population. A future research

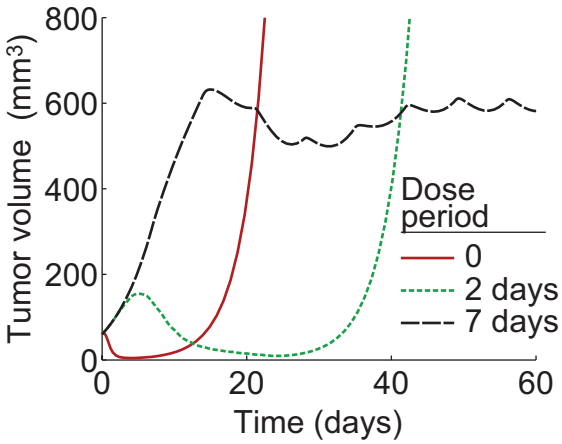

FIGURE 5. Simulations of twelve doses of virus. Twelve doses of 5×10^9 virions are injected 0, 2, or 7 days apart with the first dose beginning on day 0.

direction is to study treatment protocols as an open control problem to optimize tumor response as done in Figure 5.

3.2.3. *Stronger immune response or higher viral burst size: Maintaining an endemic infection.* Since our previous results imply that the underlying virus infection and the cytokine-stimulated immune response could have confounding effects, we considered whether increasing the immunostimulatory capability or the burst size of the virus would be more effective in reducing tumor burden. To investigate stronger immunostimulation, we increased the T cell killing constant from Table 1 by 2 and 10-fold, which gives modified values of $c_k = 1.7 \times 10^{-6}$ and $c_k = 8.5 \times 10^{-6}$. To investigate a virus with higher burst size, we increased the estimate of viral production from Table 1 by 1.1 and 1.5-fold, which gives modified values of $\alpha = 3,850$ and $\alpha = 5,250$. Figure 6 shows results of simulations using the modified parameters.

In Figure 6, we see that the two more immunostimulatory viruses with T cell killing constants increased by 2 and 10-fold cause the tumor size to decline rapidly to 33.6 mm^3 and 0.87 mm^3, respectively. However, they both lead to quick relapses, making it a less attractive strategy.

On the other hand, when viral burst sizes are increased by 10% and 50%, treatment leads to long-term equilibrium tumor populations of 139.7 mm^3 and 8.0 mm^3, respectively. These findings corroborate those of Friedman et al. [14], which also concluded that oncolytic viruses with higher burst sizes lead to long-term equilibrium tumor sizes.

What our results suggest is that designing a virus that is too highly immunogenic could have unexpected and undesirable effects on the long-term viability and strength of the oncolytic viral infection. On the other hand, developing a virus with a high burst size could lead to a treatment that can establish an endemic infection that maintains the long-term tumor and virus populations at low levels.

These observations also suggest that viruses may be used to target long-term tumor control. As a possible next step, a treatment strategy involving endemic maintenance of oncolytic virus with a more intense tumor killing strategy could be pursued.

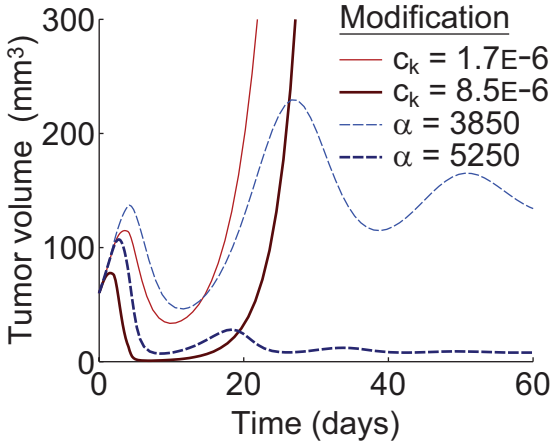

FIGURE 6. Simulations using modified Ad/4-1BBL/IL-12 viruses. Hypothetically modified viruses are more immunostimulatory or have increased viral burst size. Three doses of 5×10^9 virions are injected 2 days apart with the first dose beginning on day 0. Specific modifications in model parameters are as follows: (1) T cell killing constant increased to $c_k = 1.7 \times 10^{-6}$, (2) T cell killing constant increased to $c_k = 8.5 \times 10^{-6}$, (3) viral burst size increased to $\alpha = 3,850$, and (4) viral burst size increased to $\alpha = 5,520$.

From our simulations, we propose an approach of designing an oncolytic virus that can maintain a low-level infection and combining it with another treatment strategy aimed at tumor elimination, such as intense and temporary bursts of immunotherapy. This approach would differ from trying to directly engineer immunostimulatory capabilities into the viral genome.

3.2.4. *Specialist vs. generalist viruses.* Using our model, we considered the possibility of using a combination of the specialist viruses (Ad/4-1BBL and Ad/IL-12) instead of the generalist virus (Ad/4-1BBL/IL-12). The parameters estimated in Table 1 from fitting the model to data suggest that the Ad/4-1BBL and Ad/IL-12 viruses that are specialized to produce only one cytokine produce more stimulators of T cell and APC activity than the Ad/4-1BBL/IL-12 virus that produces both cytokines. As seen in Table 1, the T cell supply rate parameter, c_T, is 2.90 for the specialist virus Ad/4-1BBL and 1.28 for the generalist virus, Ad/4-1BBL/IL-12. Similarly, the APC recruitment rate parameter, c_A, is 1.44 for the specialist virus Ad/IL-12 and 0.22 for the generalist virus. This finding is most probably due to greater total cytokine production by cells infected by specialist viruses, consistent with Huang et al. [17], who found that the IL-12 production of Ad/4-1BBL/IL-12 is approximately half that of Ad/IL-12. Consequently, we hypothesized that a 50%-50% combination of specialist viruses will secrete more of both cytokines than a 100% dose of generalist virus. We assumed that cytokines from specialist viruses will still act synergistically to increase T cell cytotoxicity, so we set the T cell killing parameter, $c_k = 8.5 \times 10^{-7}$, for the specialist viruses to be the same as for the generalist virus. (See Table 3 for a list of parameters for the specialist viruses.)

To investigate the impact of this immunologic discrepancy on therapeutic efficacy, we compared the possibility of using the two specialist viruses, Ad/4-1BBL and Ad/IL-12, in a 50%-50% combination with the use of a 100% dose of generalist virus, Ad/4-1BBL/IL-12. The total number of virions injected was held constant at 10^{10}. Mathematically, we extended the model, equations (1)-(5) to include concurrent infections with Ad/4-1BBL and Ad/IL-12 by dividing the compartment for infected cells (B) into two equations corresponding to infection with each virus separately. We also divided the virus compartment (C) into two compartments in order to track each virus separately. Since 4-1BBL and IL-12 will act synergistically to produce a cytotoxic response with the simultaneous injection of the two specialist viruses, we used the value of the T cell killing constant, c_k, from the Ad/4-1BBL/IL-12 model. Values for the T cell and APC recruitment constants, c_T and c_A, were taken from the specialist Ad/4-1BBL and Ad/IL-12 models, respectively (see Appendix A for the modified model for the two specialist viruses).

The results of the simulated treatments are shown in Figure 7. We see that 50%-50% combinations of the specialist viruses very slightly lead to more rapid initial declines in tumor volume than 100% doses of the generalist virus. However, the specialist viruses also lead to much more rapid subsequent increases in tumor volume. We conclude that the specialist viruses Ad/4-1BBL and Ad/IL-12 do not provide a significant advantage, and may have some disadvantages, in comparison with the generalist virus Ad/4-1BBL/IL-12 considered in Huang et al. [17]. Nonetheless, this result does not preclude the possibility that alternative combinations of viruses could provide stronger effects than doses of a single homogenous virus.

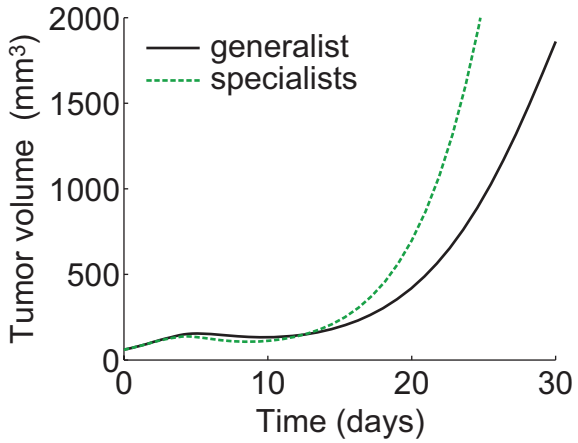

FIGURE 7. Simulations using Ad/4-1BBL/IL-12 (generalist) virus alone and Ad/4-1BBL and Ad/IL-12 (specialist) viruses in conjunction. Three doses of 5×10^9 generalist virions or $2.5\times10^9+2.5\times10^9$ specialist virions are injected 2 days apart with the first dose beginning on day 0. On day 30, the tumor volume for the simulations with generalist and specialist viruses are 1,860 mm^3 and 5,250 mm^3, respectively. In addition, the minimum tumor volumes in this period are 133 (day 9.4) and 107 mm^3 (on day 8.4), respectively. The generalist curve corresponds to the curve with period 2 days in Figure 4.

3.2.5. *Quantifying virus-mediated vs. Immune-mediated cell death.* Oncolytic virotherapy with the proposed adenoviruses has two main mechanisms of oncolysis: (i) lysis through viral replication and (ii) killing by T cell activation/stimulation from the release of IL-12 or 4-1BBL. In order to study the relative contributions to oncolysis of the two mechanisms, we calculated the proportion of cancer cells killed over time by each mechanism. Computations were carried out for unmodified Ad/4-1BBL/IL-12 virus, modified virus with T cell killing constant increased to $c_k = 8.5 \times 10^{-6}$, and modified virus with burst size increased to $\alpha = 5,520$.

From our results, it appears that lysis is the principal event in the first several days of treatment with the cytotoxic T cell response dominating thereafter (Figure 8). However, for the modified virus with increased burst size, the level of oncolysis remains elevated over the duration of the simulation (approximately 15% of cell death). In the longer term, it should be noted that a neutralizing antibody response is likely to clear the virus eventually, leaving the adaptive immune response as the major long-term contributor.

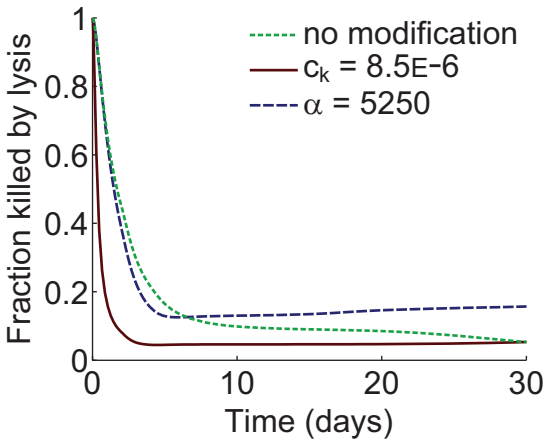

FIGURE 8. Fraction of tumor cells directly eliminated by viral infection versus T cell-mediated killing. The five curves correspond to the four curves in Figure 4 and the specialist curve in Figure 6. In all cases, oncolysis initially dominates; however, as viruses attract immune cells, dynamics progress to T cell-dominated killing.

4. **Discussion.** Oncolytic virotherapy has become a promising treatment strategy for many cancers. Oncolytic viruses that have entered clinical trials have had excellent safety profiles, demonstrating fewer off-target effects than traditional chemotherapy and radiotherapy methods (1). Unfortunately, to date, the effectiveness of oncolytic viruses has been limited, with few viruses eliciting clinically significant benefits. However, a phase III trial comparing T-VEC, a herpes simplex virus expressing GM-CSF, to GM-CSF alone for stage IIIb/c and IV melanoma has demonstrated the potential of this treatment approach. If T-VEC yields improved survival it is likely to be approved for clinical use [19]. Moreover, with the recent approval of CTLA-4 and PD-1 inhibitors as immunotherapy agents for a variety

of malignancies, future oncolytic viruses tested in the clinic are likely to incorporate similar checkpoint blockade modulation strategies [4]. Accordingly, oncolytic viruses that express these immunomodulatory factors (e.g. cytokines and cosimulatory molecules) are most likely to be incorporated into the modern anticancer arsenal.

While many cytokine and cosimulatory-molecule-expressing oncolytic viruses tested in the laboratory have the potential to proceed to clinical trials, there are an even greater number of theoretical constructs for which laboratory testing is needed, but not feasible, due to time and cost considerations. Thus, pre-laboratory, in silico methods of evaluation are needed. To this end, we have developed an ODE system describing therapy with an oncolytic adenovirus expressing 4-1BBL and IL-12 alone and in combination, with solutions fit to in vivo measurements of tumor volume (1). Parameters of the models were chosen using a nonlinear fitting scheme in MATLAB. Goodness of fit measurements revealed that the models closely approximate the true system, with R^2 values greater than 0.94 and Pearson's r correlation coefficient greater than 0.97 with all but one value greater than 0.99. The models, including the fitted parameters, were used to simulate several treatment conditions and to quantify the portions of tumor cell death attributable to oncolysis and to the cytotoxic T cell response.

We further investigated changes in tumor reduction over time due to injection of specialist viruses simultaneously, instead of injecting only the generalist virus, Ad/4-1BBL/IL-12. The specialist virus Ad/4-1BBL mediates release of 4-1BBL, while the other virus Ad/IL-12 mediates the release of IL-12. Parameter fits revealed that the specialist viruses, when used individually, mediate the release of more IL-12 or 4-1BBL than the generalist virus. Comparison of tumor reduction revealed that simultaneous injection of specialist viruses causes a slightly faster reduction in tumor burden followed by a much more rapid increase than injection of the same amount of generalist virus. Therefore, treatment with specialist viruses does not seem to be a useful tool compared with treatment with generalist viruses.

Finally, we quantified and compared the percentage of tumor cell death caused by oncolysis (i.e., through viral replication) and by T cell activation/stimulation from the release of IL-12 or 4-1BBL. We found that lysis is the principal event in the first several days of treatment, with the cytotoxic T cell response dominating thereafter.

This study represents the first mathematical model predicting the dynamics of treatment with oncolytic viruses expressing cytokines and cosimulatory molecules. The results are based on our model assumptions and would be greatly improved by validation in an experimental setting. In addition, our model is limited by its lack of spatial structure, which can influence the particular transmission patterns and therefore the results. Given that these agents may soon be approved for clinical use, the development and validation of mathematical models describing their action is needed, particularly for the elucidation of optimal therapy schemes. The model demonstrated that, while viral oncolysis is fundamental in reducing tumor burden, the increased stimulation of cytotoxic T cells leads to an even greater short-term reduction in tumor burden, but also a faster relapse.

A significant limitation in the use of virotherapy to eliminate tumors, which we also observed, is that the virus specifically infects tumor cells. When a tumor cell population becomes small, the proliferative, and thus, immunostimulatory effect of cytokine- and cotimulatory-molecule-expressing oncolytic viruses decreases

significantly, making it difficult to drive the tumor population to extinction. Our modeling revealed that combining specialist viruses, which express either IL-12 or 4-1BBL, reduces tumor burden more rapidly than the use of a generalist virus that expresses both cytokines. Accordingly, our research confirms that oncolytic viruses are useful in achieving a reduction of tumor burden, sometimes to a stable equilibrium size, and may be optimally used in combination with auxiliary treatments that can eliminate tumors completely once the tumor population is sufficiently small.

Acknowledgments. The authors received support through NSF award #1249258, the Australian Mathematical Sciences Institute, and the Society for Mathematical Biology (support for Tumor-Immune Workshop, Jan 7-10, 2013); the Australian Research Council DE120101113 (PSK); and the National Research Foundation of Korea 2013K1A1A2A02050188 (COY). In addition to the anonymous reviewers, the authors would like to thank Dr. William A. Wares and Dr. David X. Cifu for their thorough and independent reviews of the manuscript.

Appendix A. **Hierarchically fitted submodels.** This appendix contains equations and parameters for the modified model considering simultaneous treatment with the two specialist viruses Ad/4-1BBL and Ad/IL-12.

A.1. **Modified model of simultaneously injecting specialist viruses.** To examine the effects of simultaneously injecting Ad expressing the co-stimulatory molecule 4-1BB ligand (Ad/4-1BBL) and Ad expressing the immunostimulatory cytokine interleukin-12 (Ad/IL-12), we altered the previous model to account for the dynamics of the specialist viruses:

$$\frac{dU}{dt} = rU - \beta\frac{U(V_1+V_2)}{N} - k(I_1+I_2)\frac{UT}{N} \tag{6}$$

$$\frac{dI_1}{dt} = \beta\frac{UV_1}{N} - \delta_I I_1 - k(I_1+I_2)\frac{I_1T}{N} \tag{7}$$

$$\frac{dI_2}{dt} = \beta\frac{UV_2}{N} - \delta_I I_2 - k(I_1+I_2)\frac{I_2T}{N} \tag{8}$$

$$\frac{dV_1}{dt} = u_1(t) + \alpha\delta_I I_1 - \delta_V V_1 \tag{9}$$

$$\frac{dV_2}{dt} = u_2(t) + \alpha\delta_I I_2 - \delta_V V_2 \tag{10}$$

$$\frac{dT}{dt} = s_T(I_1) + pA - \delta_T T \tag{11}$$

$$\frac{dA}{dt} = s_A(I_2) - \delta_A A \tag{12}$$

- In equation (6), equation (1) has been altered to separately account for transmission due to V_1 (Ad/4-1BBL) and V_2 (Ad/IL-12). Additionally, T cells, T, at the tumor site kill uninfected cells at a frequency-dependent rate with parameter $k(I_1+I_2)$, where I_1 and I_2 are the numbers of tumor cells infected by Ad/4-1BBL and Ad/IL-12 respectively.
- Equations (7) and (8) are similar to equation (2), except that separate compartments account for the number of tumor cells infected by Ad/4-1BBl (equation (G)) and Ad/IL-12 (equation(H)).
- Similarly, equations (9) and (10) separately track the numbers of Ad/4-1BBL virions and Ad/IL-12 virions.

- In equation (11), T cell supply rate is explicitly dependent on only I_1, since we assumed only 4-1BBL affected this.
- In equation (12), the APC recruitment rate at the tumor site, $s_A(I_2)$, is explicitly dependent on only Ad/IL-12.
- Here, the total number of cells is, $N = U + I_1 + I_2 + T + A$.
- Injection of virus is done with the equation $u_1(t) = u_2(t) = 0.5u(t)$, where $u_1(t)$ and $u_2(t)$ are the injection rates of Ad/4-1BBL and Ad/IL-12, respectively.

Parameters used for this model are:

Parameter and Description		Ad/4-1BBL + Ad/IL-12 specialists	Ad/4-1BBL /IL-12 generalist
r	Net tumor growth (day^{-1})	0.31	0.31
β	Infection rate (day^{-1})	8.9×10^{-4}	8.9×10^{-4}
c_k	Kill const. (cell^{-1} day^{-1})	8.5×10^{-7}	8.5×10^{-7}
c_T	T cell constant (day^{-1})	2.9	1.28
c_A	APC constant (day^{-1})	1.44	0.22
α	Viral production	3500	3500
δ_I	Infected lysis (day^{-1})	1	1
δ_V	Viral decay (day^{-1})	2.3	2.3
δ_T	T cell decay (day^{-1})	0.35	0.35
δ_A	APC death (day^{-1})	0.35	0.35
p	T cell-APC rate (day^{-1})	1	1

TABLE 3. Table of parameters for the specialist virus model. The parameters in the generalist column are the same as those for the Ad/4-1BBL/IL-12 model in Table 1.

REFERENCES

[1] T. Alarcón, H. M. Byrne and P. K. Maini, A cellular automaton model for tumour growth in inhomogeneous environment, *J. Theor. Biol.*, **225** (2003), 257–274.

[2] N. Bagheri, M. Shiina, D. A. Lauffenburger and W. M. Korn, A dynamical systems model for combinatorial cancer therapy enhances oncolytic adenovirus efficacy by MEK-inhibition, *PLoS Comput. Biol.*, **7** (2011), e1001085.

[3] Z. Bajzer, T. Carr, K. Josić, S. J. Russell and D. Dingli, Modeling of cancer virotherapy with recombinant measles viruses, *J. Theor. Biol.*, **252** (2008), 109–122.

[4] D. L. Bartlett, Z. Liu, M. Sathaiah, R. Ravindranathan, Z. Guo, Y. He and Z. S. Guo, Oncolytic viruses as therapeutic cancer vaccines, *Mol. Cancer*, **12** (2013), p103.

[5] M. Biesecker, J. H. Kimn, H. Lu, D. Dingli and Z. Bajzer, Optimization of virotherapy for cancer, *Bull. Math. Biol.*, **72** (2010), 469–489.

[6] R. Breban, A. Bisiaux, C. Biot, C. Rentsch, P. Bousso and M. L. Albert, Mathematical model of tumor immunotherapy for bladder carcinoma identifies the limitations of the innate immune response, *Oncoimmunology*, **1** (2012), 9–17.

[7] D. M. Catron, A. A. Itano, K. A. Pape, D. L. Mueller and M. K. Jenkins, Visualizing the first 50 hr of the primary immune response to a soluble antigen, *Immunity*, **21** (2004), 341–347.

[8] Y. Chen, T. DeWeese, J. Dilley, Y. Zhang, Y. Li, N. Ramesh, J. Lee, R. Pennathur-Das, J. Radzyminski, J. Wypych, D. Brignetti, S. Scott, J. Stephens, D. B. Karpf, D. R. Henderson and D. C. Yu, CV706, a prostate cancer-specific adenovirus variant, in combination with radiotherapy produces synergistic antitumor efficacy without increasing toxicity, *Cancer Res.*, **61** (2001), 5453–5460.

[9] R. J. De Boer, M. Oprea, R. Antia, K. Murali-Krishna, R. Ahmed and A. S. Perelson, Recruitment times, proliferation, and apoptosis rates during the CD8(+) T-cell response to lymphocytic choriomeningitis virus, *J. Virol.*, **75** (2001), 10663–10669.

[10] M. Del Vecchio, E. Bajetta, S. Canova, M. T. Lotze, A. Wesa, G. Parmiani and A. Anichini, Interleukin-12: biological properties and clinical application, *Clin. Cancer Res.*, **13** (2007), 4677–4685.
[11] D. Dingli, C. Offord, R. Myers, K. W. Peng, T. W. Carr, K. Josic, S. J. Russell and Z. Bajzer, Dynamics of multiple myeloma tumor therapy with a recombinant measles virus, *Cancer Gene Ther.*, **16** (2009), 873–882.
[12] R. Eftimie, J. L. Bramson and D. J. Earn, Interactions between the immune system and cancer: A brief review of non-spatial mathematical models, *Bull. Math. Biol.*, **73** (2011), 2–32.
[13] N. B. Elsedawy and S. J. Russell, Oncolytic vaccines, *Expert Rev. Vaccines*, **12** (2013), 1155–1172.
[14] A. Friedman, J. P. Tian, G. Fulci, E. A. Chiocca and J. Wang, Glioma virotherapy: Effects of innate immune suppression and increased viral replication capacity, *Cancer Res.*, **66** (2006), 2314–2319.
[15] I. Ganly, V. Mautner and A. Balmain, Productive replication of human adenoviruses in mouse epidermal cells, *J. Virol.*, **74** (2000), 2895–2899.
[16] D. Hanahan and R. A. Weinberg, Hallmarks of cancer: The next generation, *Cell*, **144** (2011), 646–674.
[17] J. H. Huang, S. N. Zhang, K. J. Choi, I. K. Choi, J. H. Kim, M. G. Lee, M. Lee, H. Kim and C. O. Yun, Therapeutic and tumor-specific immunity induced by combination of dendritic cells and oncolytic adenovirus expressing IL-12 and 4-1BBL, *Mol. Ther.*, **18** (2010), 264–274.
[18] C. Jogler, D. Hoffmann, D. Theegarten, T. Grunwald, K. Uberla and O. Wildner, Replication properties of human adenovirus in vivo and in cultures of primary cells from different animal species, *J. Virol.*, **80** (2006), 3549–3558.
[19] H. L. Kaufman and S. D. Bines, OPTIM trial: A Phase III trial of an oncolytic herpes virus encoding GM-CSF for unresectable stage III or IV melanoma, *Future Oncol.*, **6** (2010), 941–949.
[20] N. L. Komarova and D. Wodarz, ODE models for oncolytic virus dynamics, *J. Theor. Biol.*, **263** (2010), 530–543.
[21] N. Kronik, Y. Kogan, M. Elishmereni, K. Halevi-Tobias, S. Vuk-Pavlović and A. Agur, Predicting outcomes of prostate cancer immunotherapy by personalized mathematical models, *PLoS ONE*, **5** (2010), e15482.
[22] F. Le Bœuf, C. Batenchuk, M. Vähä-Koskela, S. Breton, D. Roy, C. Lemay, J. Cox, H. Abdelbary, T. Falls, G. Waghray, H. Atkins, D. Stojdl, J. S. Diallo, M. Kærn and J. C. Bell, Model-based rational design of an oncolytic virus with improved therapeutic potential, *Nat. Commun.*, **4** (2013), p1974.
[23] F. Le Bœuf, J. S. Diallo, J. A. McCart, S. Thorne, T. Falls, M. Stanford, F. Kanji, R. Auer, C. W. Brown, B. D. and Lichty, K. Parato, H. Atkins, D. Kirn and J. C. Bell, Synergistic interaction between oncolytic viruses augments tumor killing, *Mol. Ther.*, **18** (2010), 888–895.
[24] D. Leopardo, S. C. Cecere, M. Di Napoli, C. Cavaliere, C. Pisano, S. Striano, L. Marra, L. Menna, L. Claudio, S. Perdona, S. Setola, M. Berretta, R. Franco, R. Tambaro, S. Pignata and G. Facchini, Intravesical chemo-immunotherapy in non muscle invasive bladder cancer, *Eur. Rev. Med. Pharmacol. Sci.*, **17** (2013), 2145–2158.
[25] H. L. Li, S. Li, J. Y. Shao, X. B. Lin, Y. Cao, W. Q. Jiang, R. Y. Liu, P. Zhao, X. F. Zhu, M. S. Zeng, Z. Z. Guan and W. Huang, Pharmacokinetic and pharmacodynamic study of intratumoral injection of an adenovirus encoding endostatin in patients with advanced tumors, *Gene Ther.*, **15** (2008), 247–256.
[26] D. G. Mallet and L. G. De Pillis, A cellular automata model of tumor-immune system interactions, *J. Theor. Biol.*, **239** (2006), 334–350.
[27] A. Melcher, K. Parato, C. M. Rooney and J. C. Bell, Thunder and lightning: Immunotherapy and oncolytic viruses collide, *Mol. Ther.*, **19** (2011), 1008–1016.
[28] W. Mok, T. Stylianopoulos, Y. Boucher and R. K. Jain, Mathematical modeling of herpes simplex virus distribution in solid tumors: implications for cancer gene therapy, *Clin. Cancer Res.*, **15** (2009), 2352–2360.
[29] D. M. Rommelfanger, C. P. Offord, J. Dev, Z. Bajzer, R. G. Vile and D. Dingli, Dynamics of melanoma tumor therapy with vesicular stomatitis virus: Explaining the variability in outcomes using mathematical modeling, *Gene Ther.*, **19** (2012), 543–549.
[30] S. J. Russell, K. W. Peng and J. C. Bell, Oncolytic virotherapy, *Nat. Biotechnol.*, **30** (2012), 658–670.

[31] J. R. Tysome, X. Li, S. Wang, P. Wang, D. Gao, P. Du, D. Chen, R. Gangeswaran, L. S. Chard, M. Yuan, G. Alusi, N. R. Lemoine and Y. Wang, A novel therapeutic regimen to eradicate established solid tumors with an effective induction of tumor-specific immunity, *Clin. Cancer Res.*, **18** (2012), 6679–6689.

[32] M. J. van Stipdonk, E. E. Lemmens and S. P. Schoenberger, Naïve CTLs require a single brief period of antigenic stimulation for clonal expansion and differentiation, *Nat. Immunol.*, **2** (2001), 423–429.

[33] H. Veiga-Fernandes, U. Walter, C. Bourgeois, A. McLean and B. Rocha, Response of naïve and memory CD8+ T cells to antigen stimulation in vivo, *Nat. Immunol.*, **1** (2000), 47–53.

[34] Y. Wang, H. Wang, C. Y. Li and F. Yuan, Effects of rate, volume, and dose of intratumoral infusion on virus dissemination in local gene delivery, *Mol. Cancer Ther.*, **5** (2006), 362–366.

[35] D. Wodarz, Viruses as antitumor weapons: Defining conditions for tumor remission, *Cancer Res.*, **61** (2001), 3501–3507.

[36] D. Wodarz, Computational modeling approaches to studying the dynamics of oncolytic viruses, *Math. Biosci. Eng.*, **10** (2013), 939–957.

[37] D. Wodarz and N. Komarova, Towards predictive computational models of oncolytic virus therapy: basis for experimental validation and model selection, *PLoS ONE*, **4** (2009), e4271.

[38] J. D. Wolchok, H. Kluger, M. K. Callahan, M. A. Postow, N. A. Rizvi, A. M. Lesokhin, N. H. Segal, C. E. Ariyan, R. A. Gordon, K. Reed, M. M. Burke, A. Caldwell, S. A. Kronenberg, B. U. Agunwamba, X. Zhang, I. Lowy, H. D. Inzunza, W. Feely, C. E. Horak, Q. Hong, A. J. Korman, J. M. Wigginton, A. Gupta and M. Sznol, Nivolumab plus ipilimumab in advanced melanoma, *N. Engl. J. Med.*, **369** (2013), 122–133.

[39] S. Worgall, G. Wolff, E. Falck-Pedersen and R. G. Crystal, Innate immune mechanisms dominate elimination of adenoviral vectors following in vivo administration, *Hum. Gene Ther.*, **8** (1997), 37–44.

[40] J. T. Wu, D. H. Kirn and L. M. Wein, Analysis of a three-way race between tumor growth, a replication-competent virus and an immune response, *Bull. Math. Biol.*, **66** (2004), 605–625.

[41] W. Zhang, G. Fulci, H. Wakimoto, T. A. Cheema, J. S. Buhrman, D. S. Jeyaretna, A. O. Stemmer Rachamimov, S. D. Rabkin and R. L. Martuza, Combination of oncolytic herpes simplex viruses armed with angiostatin and IL-12 enhances antitumor efficacy in human glioblastoma models, *Neoplasia*, **15** (2013), 591–599.

Received May 13, 2014; Accepted October 31, 2014.

E-mail address: pkim@maths.usyd.edu.au
E-mail address: jjc2004@med.cornell.edu
E-mail address: Il-Kyu_Choi@dfci.harvard.edu
E-mail address: chaeok@hanyang.ac.kr
E-mail address: jwares@richmond.edu